JOURNAL OF NATURAL PRODUCTS

pubs.acs.org/jnp

Article

Highly *N*-Methylated Peptides from the Antarctic Sponge *Inflatella coelosphaeroides* Are Active against *Plasmodium falciparum*

Joe Bracegirdle, Debora Casandra, James R. Rocca, John H. Adams, and Bill J. Baker*

Cite This: *J. Nat. Prod.* 2022, 85, 2454−2460

Read Online

ACCESS | Metrics & More | Article Recommendations | Supporting Information

ABSTRACT: Malaria, caused by the parasite *Plasmodium falciparum*, continues to threaten much of the world's population, and there is a pressing need for expanding treatment options. Natural products have been a vital source of such drugs, and here we report seven new highly *N*-methylated linear peptides, friomaramide B (**2**) and shagamides A−F (**3**−**8**) from the marine sponge *Inflatella coelosphaeroides*, collected in Antarctic waters, which demonstrate activity against three strains of blood-stage *P. falciparum*. The planar structures of these metabolites were solved by interpreting NMR data, as well as HRESIMS/MS fragmentation patterns, while Marfey's analysis was used to establish the configurations of the amino acids. Reisolation of the previously reported compound friomaramide A (**1**) allowed us to revise its structure. The panel of isolated compounds allowed establishing structure/activity relationships and provided information for future structure optimization for this class of *P. falciparum* inhibitory metabolites.

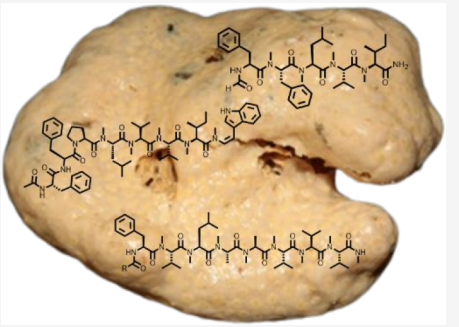

Malaria represents a serious threat to the health of a large proportion of the world's population. Despite worldwide efforts to control the disease, infections continue to increase annually, with 241 million cases and 627 000 deaths worldwide in 2020.[1] The parasite *Plasmodium falciparum* is one of the most common sources of malaria, and although several treatments exist, strains resistant to widely used drugs are spreading throughout the world.[2] Recently it has been observed that artemisinin combination therapy, which has been the gold standard for malaria treatment, is now starting to fail in some African countries.[3,4] What's more concerning is that strain resistance appears to be independent of the resistant parasite strains observed in southeast Asia, where artemisinin was first discovered and used.[4] More than 90% of malaria deaths worldwide occur in Africa alone, and there is a pressing need for completely new drugs and treatment options.[5]

Natural products are a proven source of antimalarial metabolites, with the plant-sourced quinine and artemisinin possibly the most widely appreciated to date.[6] Beyond terrestrial plants, marine organisms have also been a fruitful resource too,[7] with marine sponges leading to at least 259 unique metabolites (as of 2019) that have demonstrated anti-*P. falciparum* activity.[8]

Extreme environmental habitats of polar regions, such as that of the Southern Ocean around Antarctica, generate a huge chemical diversity within their invertebrate inhabitants.[9−11] The intense competition for scarce resources results in a need for sedentary invertebrates to acquire bioactive secondary metabolites, in order to increase chances of survival by mitigating predation, fouling, and other forms of ecological competition.[12] Annually, sponges and their biosynthetically gifted microorganisms continue to be one of the most fruitful sources for the discovery of new marine natural products,[13] including those collected from Antarctic waters.[14,15] Numerous novel peptidic natural products believed to be produced by NRPS and RIPP biosynthetic pathways have been discovered from these marine invertebrates, such as linear *N*-methylated peptides.[16−18] RHM1 and RHM2 are highly *N*-methylated octapeptides isolated from a sponge-derived *Acremonium* sp. that showed mild cytotoxic and antibacterial activity,[17] while the octapeptide pembamide isolated from a *Cribrochalina* sp. sample showed cytotoxicity against human tumor cell lines.[16] The substitution of canonical amino acids for *N*-methylated congeners has been shown to alter biological functions of polypeptides in desirable ways for the purpose of drug discovery and development, such as improved stability, binding, and oral bioavailability.[19,20] Our previous investigation of the sponge *Inflatella coelosphaeroides* following an *in vitro* liver stage malaria screen led to the isolation of friomaramide (**1**), a highly modified hexapeptide with a permethylated amide backbone and a tryptenamine residue at the C-terminus.[21] Friomaramide demonstrated significant bioactivity by blocking the liver stage of *P. falciparum* parasite development at levels comparable to the known drug primaquine.

Received: July 29, 2022
Published: September 30, 2022

https://doi.org/10.1021/acs.jnatprod.2c00684
J. Nat. Prod. 2022, 85, 2454−2460

Chart 1

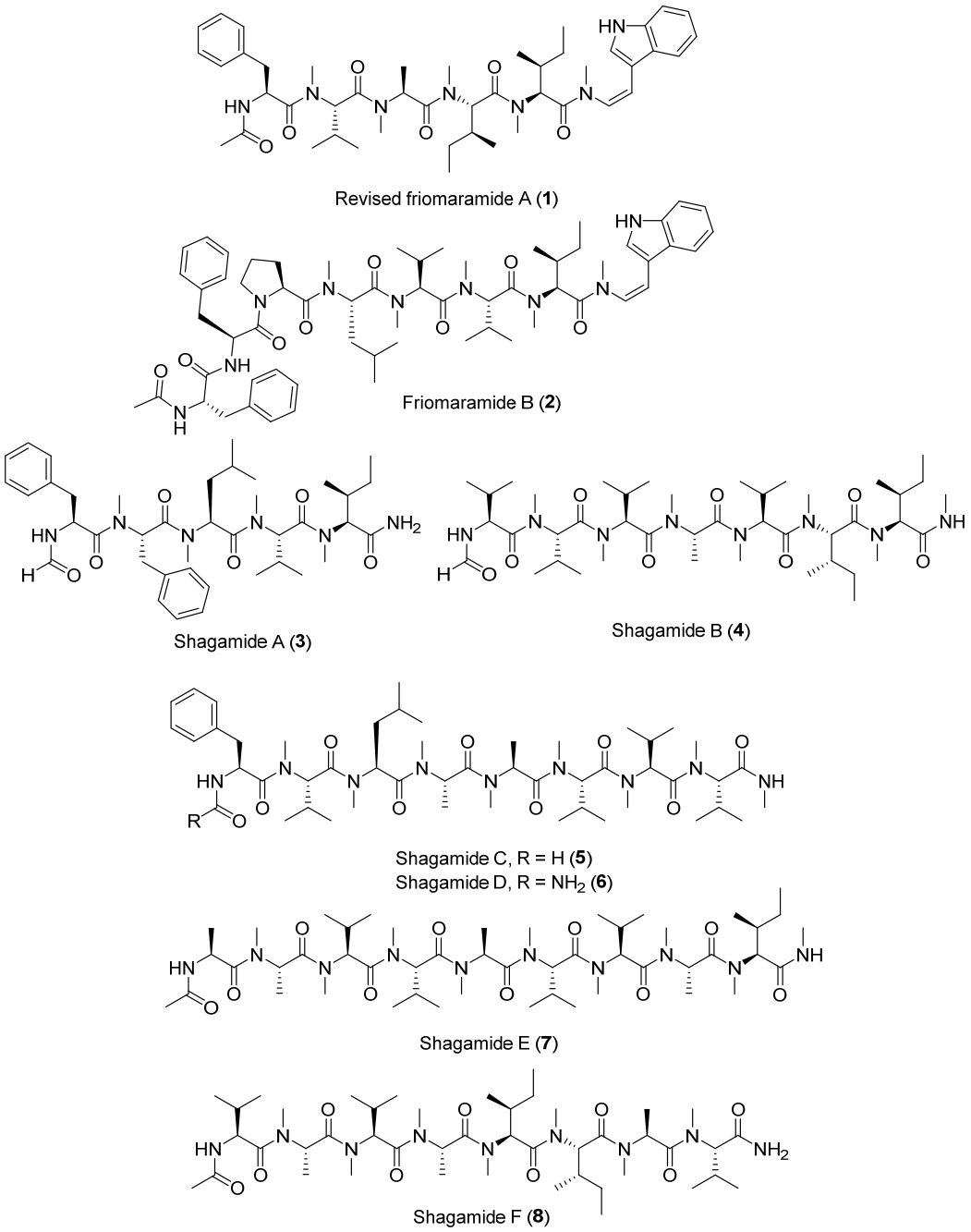

As part of our continuing investigation into the chemistry of Antarctic marine invertebrates, we turned out attention back to the sponge *I. coelosphaeroides*. Spectroscopic analysis of the unanalyzed *I. coelosphaeroides* extract fractions, along with the methanolic extract of a previously unexplored specimen, showed many signals indicative of other *N*-methylated peptides, and these were therefore subjected to a ^{1}H NMR and MS-guided isolation procedure. Through this, seven previously unreported *N*-methylated peptides were isolated, and their structures solved by a combination of NMR and MS/MS fragmentation analysis, coupled with Marfey's analysis to determine the absolute stereochemistry of the amino acids. The activity of these compounds against *P. falciparum* and their structure−activity relationships (SARs) are reported herein.

RESULTS AND DISCUSSION

The sponge *I. coelosphaeroides*, obtained from a deep-water trawl on the Scotia Arc of the Southern Ocean as previously described,[21] was freeze-dried and extracted with 1:1 CH_2Cl_2/MeOH, and the extract was fractionated by normal-phase medium-pressure liquid chromatography. The mid-polarity fractions contained metabolites bearing multiple *N*-methyl

https://doi.org/10.1021/acs.jnatprod.2c00684
J. Nat. Prod. 2022, 85, 2454−2460

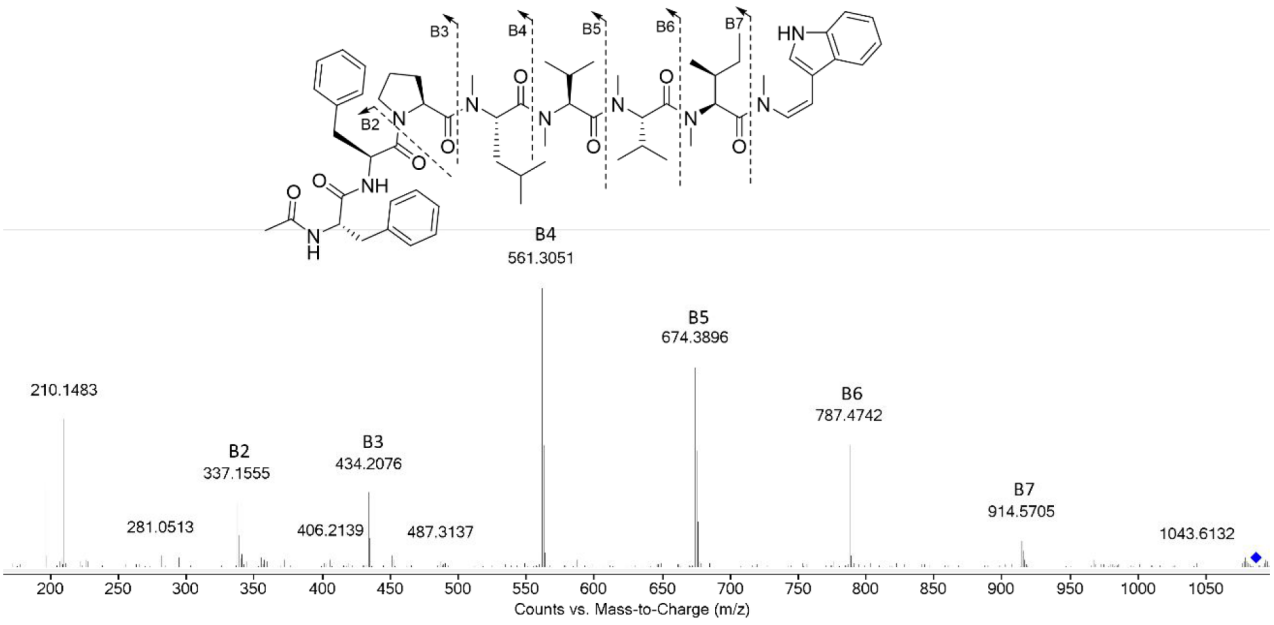

Figure 1. (+)-HRESIMS/MS (40.0 eV) fragmentation of protonated **2**.

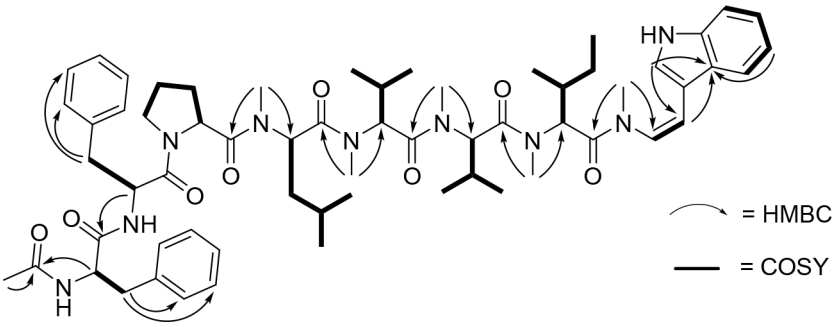

Figure 2. Key HMBC and COSY NMR correlations used for the structure elucidation of friomaramide B (**2**).

groups, reminiscent of friomaramide (friomaramide A) (**1**) and were subsequently purified by HPLC to produce seven new highly methylated peptides, including friomaramide B (**2**) and six peptides without the characteristic tryptenamine function found on friomaramides, herein named shagamides A–F (**3**–**8**).

Friomaramide B (**2**) was isolated as a white film, with a molecular formula of $C_{62}H_{87}N_9O_8$ (24 double-bond equivalents) established by analysis of the protonated molecule at *m*/*z* 1086.6729 in the (+)-HRESIMS (Figure S6). Interpretation of the ^{1}H NMR spectrum (Figure S1) in conjunction with 2D COSY, HSQC, HMBC, and HSQC-TOCSY NMR data (Table S1) suggested the presence of the proteinogenic amino acids phenylalanine (×2), proline, leucine, valine (×2), and isoleucine. Similar to friomaramide A (**1**), the data also gave evidence for five *N*-methyl groups, an acetyl group, and a decarboxylated tryptophan residue (i.e., a trypteneamine). The carbonyl and amino acid side chain groups accounted for all 24 degrees of unsaturation; therefore **2** must be linear.

The sequence of amino acids was determined by a combination of HMBC correlations (Figure S4) between neighboring residues and MS/MS fragmentation analysis (Figure S7). As with friomaramide A (**1**), the trypteneamine residue must be placed at the C-terminus due to the lack of carboxylic acid functionality. Correlations in the HMBC spectrum from the *N*-methyl at δ_H 5.49 to the olefinic C-1 (δ_C 124.6) and *N*-MeIle^7-CO (δ_C 172.3) indicated the tryptenamine nitrogen is methyl bearing and *N*-MeIle^7 is the next residue. These are both confirmed by the two fragment ions in the MS/MS spectrum at *m*/*z* 914.5705 and 787.4742 corresponding to the B7 and B6 ions, respectively (Figure 1). The process of connecting the adjacent amino acid by *N*-methyl HMBC correlations to the neighboring CO and with fragmentation data was repeated, connecting *N*-MeIle^7 to *N*-MeVal^6 followed by *N*-MeVal^5, *N*-MeLeu^4, and finally Pro^3. The N-terminus was established as acetyl-Phe^1 based on an HMBC correlation from Phe^1-α (δ_H 4.58) to the acetyl carbonyl (δ_C 172.3). The planar structure was ultimately completed by observing HMBC correlations from Phe^2-α (δ_H 4.84) to Phe^1-CO (δ_C 173.2) and the B3 MS/MS fragment *m*/*z* 434.2076 derived from acetyl-Phe^1-Phe^2-Pro^3 (Figure 2).

The olefin of the trypteneamine residue was assigned a *cis*-configuration, as the $^3J_{H,H}$ = 8.2 Hz coupling constant is consistent with other previously reported metabolites,[22,23] whereas those containing *trans*-configurations are typically much larger.[24] Stereochemical analysis using Marfey's method was then used to establish the absolute configuration of the amino acid residues in **2**.[25] A small sample of the peptide was first hydrolyzed under acidic conditions, and the resulting amino acids were derivatized with Marfey's reagent FDAA

https://doi.org/10.1021/acs.jnatprod.2c00684
J. Nat. Prod. 2022, 85, 2454–2460

(N_α-(2,4-dinitro-5-fluorophenyl-L-alaninamide). LC-HRESIMS was then used to compare the retention times of the reaction products to both D and L synthesized amino acid standards using methods previously established.[26] All of the canonical and *N*-methylated D and L amino acid isomers could be resolved using a C18 column and a linear gradient of 25% acetonitrile (ACN) (0.1% formic acid) to 100% over 40 min. By comparison of the hydrolyzed sample to the standards, this method proved all the amino acids were of the natural proteinogenic L configuration (Table S2), thus completing the 3D structure of friomaramide B (**2**).

Aside from the nature of amino acid residues, several differences between the originally proposed structure of friomaramide A (**1**) and that deduced for friomaramide B prompted reisolation and analysis of its NMR and MS data. In doing so, HMBC correlations from the signal at δ_H 3.08 to *N*-MeIle^5-CO (δ_C 172.2) and olefinic C-1 (δ_C 124.5) revealed the trypteneamine to bear an *N*-methyl group, while no methyl groups were observed to correlate with Phe^1. This was backed by the observed fragment ions in the MS/MS spectrum (Figure S58). Friomaramide A was then subjected to a stereochemical analysis using Marfey's method, where Phe^1 was determined to have the L configuration (Table S17) not D as originally proposed, while the rest of the amino acids also showed the L configuration. Thus, the revised structure of friomaramide A is consistent with that determined for friomaramide B.

Shagamide A (**3**) was isolated as a white solid, with a molecular formula of $C_{40}H_{60}N_6O_6$ inferred from the sodium adduct at *m*/*z* 743.4472 detected in the HRESIMS (Figure S13). The ^{1}H NMR spectrum (Figure S9) showed signals representative of a pentapeptide with four nitrogen-bearing methyl groups and the presence of a formyl group (δ_H 7.98, s). Correlations in the 2D NMR spectra suggested **3** was made up of an *N*-MeIle, *N*-MeVal, *N*-MeLeu, *N*-MePhe, and a Phe residue, with the HMBC from the formyl signal to α-Phe (δ_C 50.4) suggesting the only residue lacking *N*-methylation is formylated (Table S3, Figure S8). As above, HMBC correlations from the *N*-methyl ^{1}H NMR signal to the adjacent CO carbon was used alongside MS/MS fragmentation data to establish the sequence of amino acids as Phe-*N*-MePhe-*N*-MeLeu-*N*-MeVal-*N*-MeIle. Finally, the $[M - NH_2]^+$ B5 MS/MS peak at *m*/*z* 704.4382 (Figure S14) provided strong evidence for a free primary amide at the C-terminus to complete the planar structure of **3**, while the Marfey's analysis (Table S4) confirmed all amino acids were L configured.

Shagamide B (**4**) was isolated as a white solid, with a molecular formula of $C_{43}H_{80}N_8O_8$ inferred from the sodium adduct at *m*/*z* 859.6015 detected in the HRESIMS (Figure S20). Similar to **3**, the ^{1}H NMR spectrum (Figure S16) showed evidence of a heavily *N*-methylated peptide with a formyl group (δ_H 8.09, s), with 2D NMR spectra providing evidence for Val, *N*-MeVal (×3), *N*-MeIle (×2), and *N*-MeAla residues (Table S5). The order of the residues was established as Val-*N*-MeVal-*N*-MeVal-*N*-MeAla-*N*-MeVal-*N*-MeLeu-*N*-MeIle using MS/MS fragmentations as well as HMBC correlations between the *N*-methyl groups and the neighboring residues (Figure S15). The C-terminus was shown to be an *N*-methylamide, by both the HMBC correlation from the signal at δ_H 2.70 to *N*-MeIle^7-CO (δ_C 172.5) only and also the $[M - NHCH_3]^+$ B7 MS/MS peak at *m*/*z* 806.5750 (Figure S21), while the N-terminal Val was *N*-formylated, deduced by mutual HMBC correlations from the ^{1}H NMR signals of the formyl group and α-Val^1 (δ_H 4.75) to each other's ^{13}C NMR resonance (δ_C 163.4 and 54.7, respectively). Using the LC-HRESIMS Marfey's method, all the amino acids were determined to be the L isomer (Table S6). The D and L *N*-MeAla standards were inseparable using that method, but resolution of the two isomers could be achieved using the same C18 column with a gradient using H_2O and MeOH (both with 5% ACN and a 0.1% formic acid modifier, see Experimental Section),[26] facilitating comparison to the hydrolyzed shagamide B sample and confirming it as the L isomer.

Shagamide C (**5**) and shagamide D (**6**) were both isolated as white solids and share similar spectroscopic data. Shagamide C was found with a molecular formula of $C_{50}H_{85}N_9O_9$ inferred from the sodium adduct at *m*/*z* 978.6364 detected in the HRESIMS (Figure S27). By the same methods as above, **5** was found to consist of a Phe-*N*-MeVal-*N*-MeLeu-*N*-MeAla-*N*-MeAla-*N*-MeVal-*N*-MeVal-*N*-MeVal linear octapeptide, with the Phe residue formylated at the N-terminus and the C-terminus also an *N*-methylamide (Table S7). Shagamide D was found with 1D and 2D NMR data (Table S9) suggesting the same linear octapeptide backbone. However, the molecular formula of $C_{50}H_{86}N_{10}O_9$, inferred from the protonated molecule detected at *m*/*z* 971.6666 in the HRESIMS (Figure S35), has an extra NH and the ^{1}H NMR spectrum lacked a signal for the formyl group. Instead, the N-terminus is a monosubstituted ureido moiety, inferred from the ^{13}C resonance in the APT spectrum (δ_C 160.9, Figure S31), which had a similar chemical shift to previously reported peptidic natural products containing this group (e.g. anabaenopeptin 679 δ_C 158.2).[27] Also, when the NMR data were acquired in DMSO-d_6, the exchangeable NH_2 resonance (δ_H 5.57, 500 MHz) showed a ROESY correlation to Phe-NH (δ_H 6.43), thus confirming the attachment of the group to this residue (Figure S29). Application of Marfey's analysis on a hydrolyzed compound compared to synthesized standards revealed the amino acids to be all L configured for both compounds **5** and **6** (Table S8 and Table S10, respectively). The stability of compound **6** bearing a monosubstituted ureido moiety was verified by NMR and MS experiments several months following isolation and purification.

Shagamide E (**7**) was isolated as a white solid, with the molecular formula of $C_{49}H_{90}N_{10}O_{10}$ deduced from the protonated molecule detected at *m*/*z* 979.6914 in the HRESIMS (Figure S48). The amino acid sequence of Ala-*N*-MeAla-*N*-MeVal-*N*-MeVal-*N*-MeAla-*N*-MeVal-*N*-MeVal-*N*-MeAla-*N*-MeIle was determined from interpretation of the ^{1}H and ^{13}C NMR data (Table S12), with a C-terminal *N*-methylamide based on MS/MS fragmentation (Figure S49). The ^{1}H NMR spectrum (Figure S43) showed a 3H singlet at δ_H 1.95, suggestive of an acetyl functionality. Indeed, an HMBC correlation from α-Ala^1 (δ_H 4.75) to the acetyl carbonyl (δ_C 172.8) confirmed the acetyl group to be placed at the N-terminus, completing the planar structure of **7**. Shagamide F (**8**) was also isolated as a white solid, with a molecular formula of $C_{45}H_{83}N_9O_9$ inferred from the sodium adduct at *m*/*z* 916.6205 detected in the HRESIMS (Figure S56). The ^{1}H and ^{13}C NMR spectra (Figures S45, S46) suggested this compound was also acetylated at the N-terminus, while analysis of the 2D NMR spectra deduced the amino acid sequence Val-*N*-MeAla-*N*-MeVal-*N*-MeAla-*N*-MeIle-*N*-MeIle-*N*-MeAla-*N*-MeVal with a primary amide at the C-terminus. Again, the L configuration for all amino acids

https://doi.org/10.1021/acs.jnatprod.2c00684
J. Nat. Prod. 2022, 85, 2454−2460

in both **7** and **8** was determined using Marfey's method (Table S13 and Table S15, respectively).

Structurally, the friomaramides and shagamides join a rare class of natural product, each *N*-methylated across every peptide bond in the backbone. The N-termini of RiPPs and NRPs can be made up of a variety of amide caps, with acetyl groups frequently observed in both. Formyl groups have previously been observed appended to marine invertebrate-sourced peptides[28,29] and provide evidence that shagamides have an NRPs biogenesis, as no formylated RiPPs have been previously reported.[30] The monosubstituted ureido moiety present at the N-terminus of shagamide D (**6**) is extremely rare. To date, the cyanobacterial cyclic peptide anabaenopeptin 679 is the only previously reported peptidic natural product to possess this moiety,[27] and shagamide D is the first reported example with a monosubstituted ureido cap at its N-terminus.

Based on the previous observed potency of friomaramide A (**1**) against blood-state *P. falciparum*, all newly isolated compounds were screened against both sensitive (NF54 and 3D7) and resistant (Dd2) *P. falciparum* strains in the blood stage (Table 1), as well as cytotoxicity profiling (Table S18).

Table 1. IC_{50} Values (μM) of Metabolites 2−8 against Blood-Stage *P. falciparum* Strains[a]

compound	NF54	Dd2	3D7
2	3.93	3.30	8.65
3	2.61	1.72	2.10
4	>10	4.37	>10
5	3.73	1.07	2.52
6	3.05	2.02	>10
7	>10	>10	>10
8	>10	>10	>10
CQ	0.03	1.28	0.03

[a]Active compounds were tested in triplicate, while inactive ones were tested in duplicate. CQ = chloroquine.

To ensure our compounds were selective for *P. falciparum* and the results were not just simply due to cell death, the newly isolated compounds were assayed against the murine macrophage J774 cell line, where none exhibited significant cytotoxic properties as all have IC_{50} values > 20 μM.

From the initial blood-stage screen against several *P. falciparum* strains, **2**, **3**, **5**, and **6** demonstrated viable potential with activity below 10 μg/mL (<10 μM) against multiple strains, and these metabolites were prioritized for further investigation (Table 1). From these data, several key SAR features were realized. First, the rare tryptenamine C-terminal residue of friomaramide A (**1**) is not essential to activity. Although tryptenamine-bearing friomaramide B (**2**) had modest activity, shagamides **3**, **5**, and **6**, which have a hydrophobic valine or isoleucine residue C-terminus instead of tryptenamine, were generally as active or more active than friomaramide A. This suggests the mechanism of activity against *P. falciparum* is not dependent on the trypteneamine and will simplify future synthetic efforts in lead compound development. Methylation of the C-terminus amide does not appear to affect activity (namely, **3**, active but lacking C-terminus methylation). Next, it appears essential that the N-terminal amino acid residue is phenylalanine. The compounds that did not show significant activity (**4**, **7**, and **8**) all have the small hydrophobic amino acids alanine or valine in place of this residue, and this likely abrogates the observed activity. The four most active compounds did have the full variety of N-terminal amide caps that were isolated. While **5** and **6** showed similar potency against NF54 and Dd2, **5** demonstrated significant inhibition of strain 3D7 (2.52 μg/mL) and **6** was inactive, suggesting the formyl moiety is more efficacious than the primary-ureido moiety, as these two compounds only differ by this amide cap. The only other metabolite with comparable activity against the 3D7 strain was **3**, which also possessed a formyl cap; however alone this is not sufficient for activity (formylated metabolite **4** is inactive), thus providing a potential lead for future synthetic efforts. These metabolites, **2**−**6**, demonstrated promising activity against the drug-resistant strain Dd2; therefore with structure optimization they may provide a novel mechanism of action. These studies are currently ongoing in our lab.

In summary, we have discovered seven new naturally occurring linear peptides, friomaramide B (**2**) and shagamides A−F (**3**−**8**), from the Antarctic marine sponge *I. coelosphaeroides*. The isolated metabolites' differential activity against three blood-stage *P. falciparum* strains revealed the N-terminal phenylalanine residue to be essential to this activity. The compounds did not show any appreciable cytotoxic activity, and the nonbiased strain activity against chloroquine-sensitive and -resistant strains suggested a different mechanism of action. Efforts are currently underway to identify the mechanism of action, as well as synthesizing the most active compound to identify the pharmacophore and improve potency.

EXPERIMENTAL SECTION

General Experimental Procedures. Optical rotations were measured using an AutoPol IV polarimeter at 589 nm. UV/vis spectra were extracted from HPLC chromatograms. NMR spectra were acquired using either a Varian Inova 500 spectrophotometer or a Bruker Bio-Spin 800 MHz spectrophotometer equipped with a 5 mm TXI cryoprobe. The residual solvent peak was used as an internal chemical shift reference (CD_3OD: δ_C 49.0; δ_H 3.31, DMSO-d_6: δ_C 39.52; δ_H 2.50). High-resolution mass spectrometry/liquid chromatography data were obtained on an Agilent 6540 QTOF LCMS with electrospray ionization detection. Medium-pressure liquid chromatography (MPLC) was performed using a Combiflash Rf 200i MPLC, using ELSD and UV detection with a RediSepRf 80 g silica column. Reversed-phase HPLC was performed on a Shimadzu LC20-AT system equipped with a photodiode array detector (M20A) using a semipreparative Phenominex C18 column (10 μm, 100 Å, 250 × 10 mm; 4 mL/min) or on an analytical Phenomenex polar C18 column (5 μm, 100 Å, 250 × 4.6 mm; 1 mL/min). All solvents used for column chromatography were of HPLC grade, and H_2O was distilled. Solvent mixtures are reported as % v/v unless otherwise stated.

Biological Material, Extraction, and Isolation. The *Inflatella coelosphaeroides* specimens and their identification used for this study were described in detail in our previous study.[21] The remaining sponge fractions of interest generated in the initial study were combined and analyzed by LCMS. Briefly, a collection of *I. coelosphaeroides* sponge samples was extracted twice overnight in 1:1 CH_2Cl_2/MeOH. The extracts were dried and mounted onto silica gel and then partitioned using NP flash MPLC with a gradient from hexane to EtOAc and washed with 20% MeOH in EtOAc. Friomaramide A (**1**) was isolated from the E fraction eluting at 20% MeOH in EtOAc, so the remaining E side-fractions alongside those of F were combined to generate "Extract 2021". Extract 2021 (70 mg) was fractionated with semipreparative C18 HPLC (4 mL/min), using a linear gradient from 10% MeOH/H_2O to 100% MeOH over 60 min, generating fractions 1−16. The individual fractions were then purified again by C18 HPLC (4 mL/min) this time using a linear gradient from 10% ACN/H_2O to 100% ACN over 60 min, and finally

https://doi.org/10.1021/acs.jnatprod.2c00684
J. Nat. Prod. 2022, 85, 2454−2460

cleaned by analytical polar C18 HPLC (1 mL/min) using a linear gradient from 50% MeOH/H_2O to 100% MeOH over 60 min to afford the pure peptides friomaramide B (0.60 mg), shagamide A (1.05 mg), shagamide B (0.80 mg), shagamide C (1.15 mg), shagamide D (1.05 mg), shagamide E (1.40 mg), and shagamide F (1.25 mg).

*Friomaramide B (**2**):* white solid; $[\alpha]^{22}_D$ −17.4 (*c* 0.05, MeOH); UV (MeOH) λ_{max} 221, 280 nm; ^{1}H and ^{13}C NMR (CD_3OD) Table S1; HRESIMS *m*/*z* 1086.6729 $[M + H]^+$ (calcd for $C_{62}H_{88}N_9O_8$, 1086.6750; Δ −1.93 ppm).

*Shagamide A (**3**):* white solid; $[\alpha]^{22}_D$ −151.4 (*c* 0.05, MeOH); UV (MeOH) λ_{max} 215, 275 nm; ^{1}H and ^{13}C NMR, see Table S3; HRESIMS *m*/*z* 743.4472 $[M + Na]^+$ (calcd for $C_{40}H_{60}N_6O_6Na$, 743.4467; Δ 0.67 ppm).

*Shagamide B (**4**):* white solid; $[\alpha]^{22}_D$ −66.6 (*c* 0.05, MeOH); UV (MeOH) λ_{max} 220, 280 nm; ^{1}H and ^{13}C NMR, see Table S5; HRESIMS *m*/*z* 859.6015 $[M + Na]^+$ (calcd for $C_{43}H_{80}N_8O_8Na$, 859.5991; Δ 2.79 ppm).

*Shagamide C (**5**):* white solid; $[\alpha]^{22}_D$ −196.6 (*c* 0.05, MeOH); UV (MeOH) λ_{max} 215 nm; ^{1}H and ^{13}C NMR, see Table S7; HRESIMS *m*/*z* 978.6364 $[M + Na]^+$ (calcd for $C_{50}H_{85}N_9O_9Na$, 978.6362; Δ 0.20 ppm).

*Shagamide D (**6**):* white solid; $[\alpha]^{22}_D$ −166.6 (*c* 0.05, MeOH); UV (MeOH) λ_{max} 215, 275 nm; ^{1}H and ^{13}C NMR, see Table S9; HRESIMS *m*/*z* 971.6666 $[M + H]^+$ (calcd for $C_{50}H_{87}N_{10}O_9$, 971.6652; Δ 1.44 ppm).

*Shagamide E (**7**):* white solid; $[\alpha]^{22}_D$ −214.0 (*c* 0.05, MeOH); UV (MeOH) λ_{max} 215 nm; ^{1}H and ^{13}C NMR, see Table S12; HRESIMS *m*/*z* 979.6914 $[M + H]^+$ (calcd for $C_{49}H_{91}N_{10}O_{10}$, 979.6914; Δ 0 ppm).

*Shagamide F (**8**):* white solid; $[\alpha]^{22}_D$ −150.6 (*c* 0.05, MeOH); UV (MeOH) λ_{max} 215, 275 nm; ^{1}H and ^{13}C NMR, see Table S14; HRESIMS *m*/*z* 916.6205 $[M + H]^+$ (calcd for $C_{45}H_{83}N_9O_9Na$, 916.6206; Δ −0.11 ppm).

Stereochemical Analysis Using Marfey's Method. A 0.1 mg sample of peptides **2**−**8** was individually hydrolyzed with 200 μL of 6 N HCl at 100 °C for 12 h. The hydrolysate was then evaporated to dryness under a stream of N_2 overnight and then lyophilized for 1 h to remove residual HCl. It was then suspended in 100 μL of H_2O and treated with 50 μL of saturated $NaHCO_3$(aq) and 200 μL of 1% FDAA in acetone. The solution was stirred at 40 °C for 1 h before being quenched with 50 μL of 1 M HCl. Next 250 μL of ACN was added, and it was passed through a syringe filter and analyzed by LCMS. A 1 μL injection of the solution was run on a Kinetex C18 column (2.6 μm, 100 Å, 150 × 3 mm; 0.5 mL/min) using two methods individually: first, a linear gradient from 25% ACN/H_2O (0.1% HCO_2H) to 100% ACN/H_2O (0.1% HCO_2H) over 40 min, and second an isocratic elution of 20% ACN/H_2O (0.1% HCO_2H, 5% ACN) for 20 min followed by a linear gradient to 40% ACN/H_2O (0.1% HCO_2H, 5% ACN) over 20 min (to get separation of *N*-MeAla isomers). The amino acid content of the hydrolysate was assessed by monitoring the (+)-HRESIMS, and the EIC retention times were compared to standards synthesized and analyzed by the same method.

Cytotoxicity Assay. The isolated compounds were each tested for cytotoxicity using mammalian J774A.1 cell lines (ATCC TIB-67) in complete media and RPMI 1640 medium with phenol red containing L-glutamine and then supplemented with 10% fetal bovine serum (CM). Cells were seeded at 5 × 10^5 cell/mL, plated in a 96-well format with 100 μL/well fresh media on day 0, and incubated overnight at 37 °C, 5% CO_2 for adherence. Following 24 h of incubation, spent media was removed, and 100 μL of fresh media with test compounds serially diluted 1:2 with a starting concentration of 10 μg/mL was added to the cells and incubated for an additional 68 h before adding in 20 μL of CellTiter 96 AQueous One Solution Cell Proliferation Assay reagent (Promega). Cells were incubated for an additional 4 h before reading absorbance (490) nm on the CLARIOstar plate reader.

Blood-Stage Antiplasmodial Assay. For parasite suspension, *P. falciparum* malaria strains were grown under normal conditions as previously described by Trager and Jensen with some modifications.[31] Briefly, parasites were suspended in RPMI 1640, supplemented with 0.23% sodium bicarbonate, 50 mg/mL hypoxanthine, and 0.5% albumax (CM), and 4% packed washed red blood cells by volume and incubated in a continuous gas incubator set to normal conditions (5% O_2, 5% CO_2, 95% N). Parasites were prepared for drug susceptibility assay by highly synchronizing schizonts 16 h before experiment start by using a 70% Percoll method. Ring stage parasites were then resuspended in culture with fresh CM containing 2% hematocrit and 0.5% parasitemia.

Antimalaria activity was assessed against reference strains of NF54, 3D7, and Dd2 using an adaptation of the sensitivity assay of Desjardins et al. using SybrGreen fluorescence as an assessment of parasite growth.[32] NF54 original isolate obtained from a patient living near Schiphol Airport, Amsterdam, and its clonal isolate 3D7 are generally considered to be drug sensitive, though 3D7 does convey resistance to sulfadoxine. Dd2 derived from the parent W2 is a multidrug-resistant line originating from the Indochina III/CDC isolate, which contains point mutations in *pfcrt* as well as amplifications in *pfmdr1* and GTP cyclohydrolase. Briefly, compounds were diluted to 10 μg/mL and serially diluted along a microtiter plate before adding in 100 μL/well of the parasite suspension. Parasite growth was compared to controls incubated at 37 °C and normal culture conditions (5% O_2, 5% CO_2, 90% N_2) for 72 h. Plates were frozen and thawed before adding a final 1× concentration of SybrGreen in lysis buffer and read on the CLARIOstar fluorescence plate reader (Ex/Em 484-15/528-15) following a 45 min incubation at room temperature. Drug EC_{50} values were calculated by interpolation of the probit transformation of the log(dose)−response curve using the MARS software provided by BMG.

■ ASSOCIATED CONTENT

Supporting Information

The Supporting Information is available free of charge at https://pubs.acs.org/doi/10.1021/acs.jnatprod.2c00684.

NMR and HRESIMS spectra, as well as cytotoxicity data for metabolites **2**−**8** (PDF)

■ AUTHOR INFORMATION

Corresponding Author

Bill J. Baker − *Department of Chemistry, University of South Florida, Tampa, Florida 33620, United States;* orcid.org/0000-0003-3033-5779; Email: bjbaker@usf.edu

Authors

Joe Bracegirdle − *Department of Chemistry, University of South Florida, Tampa, Florida 33620, United States*

Debora Casandra − *Center for Global Health and Infectious Disease Research, College of Public Health, University of South Florida, Tampa, Florida 33612, United States*

James R. Rocca − *AMRIS, McKnight Brain Institute, University of Florida, Gainesville, Florida 32610, United States*

John H. Adams − *Center for Global Health and Infectious Disease Research, College of Public Health, University of South Florida, Tampa, Florida 33612, United States*

Complete contact information is available at: https://pubs.acs.org/10.1021/acs.jnatprod.2c00684

Notes

The authors declare no competing financial interest.

■ ACKNOWLEDGMENTS

This work was supported by the National Science Foundation awards PLR-1341339 (B.J.B.) and ANT-1043749 (to Nerida G. Wilson, Western Australia Museum) from the Antarctic

Organisms and Ecosystems Program. We thank the crew and research scientists on board the *Nathaniel B. Palmer* for assistance during the research cruise. A portion of this work was performed in the McKnight Brain Institute at the National High Magnetic Field Laboratory's Advanced Magnetic Resonance Imaging and Spectroscopy (AMRIS) Facility, which is supported by National Science Foundation Cooperative Agreement DMR-1644779 and the State of Florida. Nerida G. Wilson and Greg W. Rouse, Scripps Institution of Oceanography, were instrumental in the logistical and conceptual implementation of this research.

REFERENCES

(1) WHO World malaria report 2021. https://www.who.int/teams/global-malaria-programme/reports/world-malaria-report-2021.
(2) Jagannathan, P.; Kakuru, A. *Nat. Commun.* **2022**, *13* (1), 2678.
(3) Tindana, P.; de Haan, F.; Amaratunga, C.; Dhorda, M.; van der Pluijm, R. W.; Dondorp, A. M.; Cheah, P. Y. *Malaria J.* **2021**, *20* (1), 119.
(4) Owoloye, A.; Olufemi, M.; Idowu, E. T.; Oyebola, K. M. *Malaria J.* **2021**, *20* (1), 451.
(5) Fidock, D. A.; Rosenthal, P. J. *Med.* **2021**, *2* (12), 1287−1288.
(6) Tajuddeen, N.; Van Heerden, F. R. *Malaria J.* **2019**, *18* (1), 404.
(7) Hai, Y.; Cai, Z.-M.; Li, P.-J.; Wei, M.-Y.; Wang, C.-Y.; Gu, Y.-C.; Shao, C.-L. *Nat. Prod. Rep* **2022**, *39* (5), 969−990.
(8) Aguiar, A. C. C.; Parisi, J. R.; Granito, R. N.; de Sousa, L. R. F.; Renno, A. C. M.; Gazarini, M. L. *Mar. Drugs* **2021**, *19* (3), 134.
(9) Lebar, M. D.; Heimbegner, J. L.; Baker, B. J. *Nat. Prod. Rep* **2007**, *24* (4), 774−797.
(10) Soldatou, S.; Baker, B. J. *Nat. Prod. Rep* **2017**, *34*, 585−626.
(11) Núñez-Ponz, L.; Shilling, A. J.; Verde, C.; Baker, B. J.; Giordano, D. *Mar. Drugs* **2020**, *18*, 401.
(12) Núñez-Pons, L.; Avila, C. *Nat. Prod. Rep* **2015**, *32* (7), 1114−1130.
(13) Carroll, A. R.; Copp, B. R.; Davis, R. A.; Keyzers, R. A.; Prinsep, M. R. *Nat. Prod. Rep* **2021**, *38* (2), 362−413.
(14) Shilling, A. J.; Witowski, C. G.; Maschek, J. A.; Azhari, A.; Vesely, B.; Kyle, D. E.; Amsler, C. D.; McClintock, J. B.; Baker, B. J. *J. Nat. Prod* **2020**, *83*, 1553−1562.
(15) Li, F.; Pandey, P.; Janussen, D.; Chittiboyina, A. G.; Ferreira, D.; Tasdemir, D. *J. Nat. Prod* **2020**, *83* (3), 706−713.
(16) Urda, C.; Pérez, M.; Rodríguez, J.; Jiménez, C.; Cuevas, C.; Fernández, R. *Tetrahedron Lett.* **2016**, *57* (30), 3239−3242.
(17) Boot, C. M.; Tenney, K.; Valeriote, F. A.; Crews, P. *J. Nat. Prod* **2006**, *69* (1), 83−92.
(18) Dewapriya, P.; Khalil, Z. G.; Prasad, P.; Salim, A. A.; Cruz-Morales, P.; Marcellin, E.; Capon, R. J. Talaropeptides A-D: Structure and biosynthesis of extensively *N*-methylated linear peptides from an Australian marine tunicate-derived *Talaromyces* sp. *Front. Chem.*. **2018**, *6*, DOI: 10.3389/fchem.2018.00394.
(19) Nabika, R.; Oishi, S.; Misu, R.; Ohno, H.; Fujii, N. *Bioorg. Med. Chem.* **2014**, *22* (21), 6156−6162.
(20) Biron, E.; Chatterjee, J.; Ovadia, O.; Langenegger, D.; Brueggen, J.; Hoyer, D.; Schmid, H. A.; Jelinek, R.; Gilon, C.; Hoffman, A.; Kessler, H. *Angew. Chem. Internat. Ed* **2008**, *47* (14), 2595−2599.
(21) Knestrick, M. A.; Wilson, N. G.; Roth, A.; Adams, J. H.; Baker, B. J. *J. Nat. Prod* **2019**, *82* (8), 2354−2358.
(22) Izumikawa, M.; Hashimoto, J.; Takagi, M.; Shin-ya, K. *Aspergillus sp. SpD081030G1f1. J. Antibiot* **2010**, *63*, 389−391.
(23) Ondeyka, J. G.; Dombrowski, A. W.; Polishook, J. P.; Felcetto, T.; Shoop, W. L.; Guan, Z.; Singh, S. B. *J. Ind. Microbiol. Biotechnol* **2003**, *30* (4), 220−224.
(24) Palermo, J. A.; Flower, P. B.; Seldes, A. M. *Tetrahedron Lett.* **1992**, *33* (22), 3097−3100.
(25) Harada, K.-i.; Fujii, K.; Mayumi, T.; Hibino, Y.; Suzuki, M.; Ikai, Y.; Oka, H. *Tetrahedron Lett.* **1995**, *36* (9), 1515−1518.
(26) Vijayasarathy, S.; Prasad, P.; Fremlin, L. J.; Ratnayake, R.; Salim, A. A.; Khalil, Z.; Capon, R. J. *J. Nat. Prod* **2016**, *79* (2), 421−427.
(27) Harms, H.; Kurita, K. L.; Pan, L.; Wahome, P. G.; He, H.; Kinghorn, A. D.; Carter, G. T.; Linington, R. G. *Bioorg. Med. Chem. Lett.* **2016**, *26* (20), 4960−4965.
(28) Fukuhara, K.; Takada, K.; Okada, S.; Matsunaga, S. *J. Nat. Prod* **2016**, *79* (6), 1694−1697.
(29) Kobayashi, J.; Cheng, J.; Ohta, T.; Nakamura, H.; Nozoe, S.; Hirata, Y.; Ohizumi, Y.; Sasaki, T. *J. Org. Chem.* **1988**, *53* (26), 6147−6150.
(30) Wenski, S. L.; Thiengmag, S.; Helfrich, E. J. N. *Synth. Syst. Biotechnol* **2022**, *7* (1), 631−647.
(31) Trager, W.; Jensen, J. B. *Science* **1976**, *193* (4254), 673−675.
(32) Desjardins, R. E.; Canfield, C. J.; Haynes, J. D.; Chulay, J. D. *Antimicrob. Agents Chemother.* **1979**, *16* (6), 710−718.